



Published in final edited form as:

Mol Pharm. 2009 ; 6(3): 873–882. doi:10.1021/mp800197v.

Affinity of Drugs and Small Biologically Active Molecules to Carbon Nanotubes: A Pharmacodynamics and Nanotoxicity Factor?

John Liu[§], Liu Yang[&], and Anton J. Hopfinger^{#,§,*}

[§]The Chem21 Group, Inc. 1780 Wilson Drive Lake Forest, IL 60045

[&]Department of Chemistry & Biochemistry University of Delaware Newark, DE 19711

[#]College of Pharmacy MSC09 5360 1 University of New Mexico Albuquerque, NM 87131-0001

Abstract

The MM-PBSA MD method was used to estimate the affinity, as represented by $\log k_b$, of each of a variety of biologically active molecules to a carbon nanotube in an aqueous environment. These ligand-receptor binding simulations were calibrated by first estimating the $\log k_b$ values for eight ligands to human serum albumin, HSA, whose $\log k_b$ values have been observed. A validation linear correlation equation was established [$R^2 = 0.888$ $Q^2 = 0.603$] between the observed and estimated $\log k_b$ values to HSA. This correlation equation was then used to re-scale all MM-PBSA MD $\log k_b$ values using a carbon nanotube as the receptor. The $\log k_b$ of the eight HSA ligands, nine polar and/or rigid ligands and six nonpolar and/or flexible ligands to a carbon nanotube were estimated. The range in re-scaled $\log k_b$ values across this set of 23 ligands is 0.25 to 7.14, essentially seven orders of magnitude. Some ligands, like PGI₂, bind in the $\log k_b = 7$ range which corresponds to the lower limits of known drugs. Thus, such significant levels of binding of biologically relevant compounds to carbon nanotubes might lead to alterations in the normal pharmacodynamic profiles of these compounds and be a source of toxicity. Ligand binding potency to a carbon nanotube is largely controlled by the shape, polarity/nonpolarity distribution and flexibility of the ligand. HSA ligands exhibit the most limited binding to a carbon nanotube, and they are relatively rigid and of generally spherical shape. Polar and/or rigid ligands bind less strongly to the carbon nanotube, on average, than nonpolar and/or flexible ligands even though the chosen members of both classes of ligands in this study have chain-like shapes that facilitate binding. The introduction of only a few strategically spaced single bonds in the polar and/or rigid ligands markedly increases their binding to a carbon nanotube.

Keywords

molecular dynamics; drug binding; carbon nanotubes; nanotoxicity; pharmacodynamics

Introduction

Research into the toxicity of nanomaterials, generally referred to as “nanotoxicity”^{1, 2}, is being carried out, but at a far slower pace than research into how nanomaterials can be employed³⁻⁵. Significant future efforts in nanotoxicity are going to be required in order to discern the effects that nanoscale materials may have on humans and the environment^{6, 7}. However, it is not clear how to develop an arsenal of meaningful and reliable nanotoxicity

*Corresponding author: Email: hopfingr@unm.edu, Voice: 505.272.8474 Fax : 505.272.0704 .

screens and assays⁸. One approach to consider as a member of the arsenal is to perform simulation and modeling experiments which explore the behavior of nanomaterials in relevant biological settings. These simulation and modeling studies could serve as prescreens to identify the more likely sources and mechanisms of nanotoxicity.

Carbon nanotubes are among the currently most popular nanomaterials, and are being evaluated for a wide variety of possible applications. Toxicology studies of the effects of carbon nanotubes have been performed since 2003⁹. However, the results are relatively few, and it is not possible to make full conclusions and accurate human assessments. There have been some recent studies showing the promise in the use of carbon nanotubes for biomedical applications that included exploration of possible toxic side effects¹⁰⁻¹³. As part of one related investigation of this type, it was found that after injecting mice with single-walled carbon nanotubes, “near-complete clearance [of the nanotubes] from the main organs in 2 months” and “no toxic side effects” were observed¹⁴. While these new findings are encouraging, other reports have suggested that nanotubes cause pulmonary damage to the lungs of mice and alter protein expression^{15, 16}. In addition, it has been reported that carbon nanotubes adsorb essential micronutrients¹⁷.

One of the applications of carbon nanotubes being explored is as selective membrane channels^{18, 19}. The carbon nanotube is inserted across a cellular membrane in order to selectively transport agents in and out of cells. Recently we have performed simulation and modeling experiments to determine what changes in cellular membrane structure and function can occur due to the insertion of carbon nanotubes across the membrane. The results of our study²⁰ indicate four types of changes in the properties of the membrane bilayer;

1. The structural organization and packing of the constituent phospholipids of the membrane bilayer are markedly altered.
2. The dynamical features of the membrane bilayer are altered with the membrane becoming more rigid.
3. The transport characteristics of small polar molecules across the membrane bilayer are altered with respect to both permeation rate and transport direction.
4. The transport of solvated ions through the inserted nanotube alters, selectively, the structural organization of the surrounding membrane bilayer.

A general consideration when exploring the possible toxicity of a drug-candidate is to investigate its binding propensity to sites other than to the receptor it is designed to engage²¹. Not all such *secondary* binding is bad, and, in fact, such secondary binding is sometimes useful in delivering the drug candidate to the location of its targeted receptor. But, generally, the more specific and selective is the binding of the drug candidate to only its receptor site, the safer is the drug candidate. In the case of exploring sources of nanotoxicity, the nanoparticle now becomes a possible new receptor site to which drugs and/or other small biologically significant compounds might unexpectedly bind. The binding of a particular drug or biologically significant compound to a nanoparticle may not lead to toxicity, but the possibility necessitates being able to determine if such binding is indeed possible, and to what extent it might occur.

The objectives of the work reported in this paper were a) to develop a molecular modeling and computational scheme to estimate the binding constants of drugs and small biological compounds to carbon nanotubes, and, b) to compare these binding constants to those observed for drugs binding to a known drug carrier protein, namely human serum albumin, HSA^{22, 23}. The known low to medium affinity range of HSA ligands is the same affinity range one would expect for relatively non- to semi-specific ligand-receptor binding as

presented by a carbon nanotube to an arbitrary ligand. Thus, comparative and validation use of the HSA-ligand system constitutes a relevant, reliable and appropriate approach to accomplish the objectives in modeling carbon nanotube- ligand binding.

By being able to estimate the binding constants of drugs and other biologically significant molecules to nanotubes, and then comparing them to known ligand binding constants to HSA, one is in a position to meaningfully postulate which drugs and biological molecules will have their pharmacodynamic profiles²⁴ most influenced by the presence of carbon nanotubes. The alteration of a pharmacodynamic profile of a drug, and/or biologically relevant small molecule, in turn, can be used as a caution flag [pre-screen] for possible nanotoxicity, and thereby signal the need for expanded toxicological testing. Of course, this reasoning assumes that the carbon nanotubes are present in sufficient concentrations to fully realize the pharmacological effects of ligands binding to them.

Method

The biophysical environment assumed in performing the simulation studies reported here is that, at a minimum, a significantly large area of a carbon nanotube surface is exposed to a ligand in an aqueous media to realize the most favorable binding of the ligand to the nanotube. The overall strategy to estimate the binding constants of drugs and small biologically relevant molecules to carbon nanotubes consists of the following steps;

1. Identify the available set of ligands to HSA for which both the binding geometry and binding constant are known are each ligand.
2. Perform a solvent-dependent molecular dynamics based docking study for each ligand to HSA and estimate the corresponding thermodynamic properties and binding constant.
3. Compare, including construction of a linear regression fit, the estimated and observed binding constants of the set of ligands to HSA. This step constitutes a validation of the solvent-dependent molecular dynamics based docking method and also permits the re-scaling of the estimated binding constants to the observed binding constants.
4. Repeat the solvent-dependent molecular dynamics based docking studies, but for ligands of interest binding to the carbon nanotube in an aqueous environment.
5. Re-scale the estimated binding constants for the ligands to the carbon nanotube using the linear regression fit established in step 3 above.

The structure of the carbon nanotube is well-defined owing to its rigidity, and the periodicity in the chemical structure of the carbon nanotube is quite limited and correspondingly permits a full exploration of plausible initial binding modes between a ligand and carbon nanotube. Moreover, validation of the binding estimation methodology on a much more complex system in terms of both 3D-chemical structure and range in atom diversity of the receptor, namely HSA, supplies confidence that the methodology will work using the carbon nanotube as the 'receptor'. The details on each of the components of the methodology involved in this study are as follows;

- A. *The HSA Ligands* : The set of ligands whose binding constants and bound crystal structures to HSA are known are given in Table 1. In those cases, like propofol, where multiple modes of binding to HSA are reported²², the binding geometry and corresponding binding constant of the low 'physiological ligand concentration' has been used. There is also the consideration that serum drug concentration, and serum variation in HSA concentration, can both modulate the clinical binding behavior of

a drug. However, the binding data used in this work is completely limited to *in vitro* measurements.

- B.** *The Carbon Nanotube:* An uncapped, single-walled nanotube 50 Å long, having a diameter of 10 Å was constructed based upon the method developed by Lopez and coworkers¹⁹. This nanotube is identical to that used in our previous study of the insertion of a nanotube into a DMPC bilayer²⁰.
- C.** *Selection of Initial Docking Geometries:* The initial docking geometries used for the MD binding simulations of the ligands to HSA are the crystal structures of the HSA-ligand complexes relaxed to eliminate any bad atom-pair contacts. The relaxation process was constrained to minimize the sum of the squares of the distances between locations of the atoms of the crystal structure and those in the relaxed structure.

A carbon atom in the ‘center’ of the carbon nanotube with respect to its length was chosen as a reference docking atom for each of the set of ligands to be bound to the carbon nanotube. A set of 30 of different randomly selected locations and poses were chosen about this carbon atom such that the relative locations were not greater than one C-C bond length from the carbon, and no bad atom-pair contacts were realized between the ligand and carbon nanotube for the choices in both location and pose.

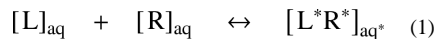
- D.** *Solvent-Dependent Molecular Dynamics Docking:* The molecular mechanics - Poisson-Boltzmann solvent accessible surface area (MM-PBSA)²⁵ molecular dynamics (MD) method, as implemented in AMBER 9^{26, 27}, was employed to calculate the binding free energies of the ligands to both HSA and the carbon nanotube. MD simulations using an implicit solvent model were selected in order to make the computations tractable for reliably handling a relatively large number of ligand-receptor systems. In particular, the MM-PBSA MD method permits faster equilibration times, easily tunable solvent properties, and, shorter computation cycles than most other equivalent MDS methods.

The SANDER module of the AMBER 9 package and the updated version of the PAM1 parameters were used in the MD simulations²⁷. Constant pressure simulations (NTP) were run at a time step of 100 ps. These simulations were carried out at a temperature of 298 K with Berendsen temperature coupling. Electrostatic interactions were computed with the Particle Mesh Ewald method implemented in SANDER. The Lenard-Jones interactions were evaluated with an 8.0 Å cutoff value. The non-bonded pair list was updated every 100 MDS steps. After the initial 1000 steps of energy minimization, the system was equilibrated during a 100 ps of MD run with positional constraints. During the first 20 ps of the equilibration, the system was heated from 0 to 298 K. The positional constraints were gradually reduced from 50 to 0.5 kcal/(mol Å) within equilibration time. The production MD simulations (without positional constraints) were run for 500 ps. Generated structures were stored in trajectory files every 0.1 ps, providing 5,000 sampled states for each run. The collected structural data were analyzed with the MM-PBSA module of the AMBER 9 software to calculate binding affinity. Additional details and theory regarding the use of MM-PBSA to calculate a binding affinity measure are given in the cited references^{26,27}.

It is important to point out that in the MM-PBSA approach considerable attention has been devoted to adjusting model parameters, such as atomic radii and solute dielectric constant, to reproduce experimental observations. This approach is in contrast to attempting to develop more physical (and complex) implicit solvent representations. The PBSA approach affords an accuracy that is comparable, or

even superior, to explicit solvent simulation methods if the parameters are properly chosen.

The overall objective of the MM-PBSA method is to calculate the free energy difference between two states which, in this analysis, correspond to the bound and unbound states of the ligand as expressed by the linear product equation;



In eq. (1) L stands of unbound ligand, R the unbound receptor and L^*R^* the bound complex. The aq indicates all states include an aqueous medium.

The binding constant for a given ligand-receptor system is determined directly from the binding free energy difference between the bound and unbound states computed from employing the MM-PBSA MD method.

- E. Selection of Ligands for Binding to the Carbon Nanotube:** All of the HSA ligands were included in the overall set of compounds with their binding to the carbon nanotube estimated using the MM-PBSA MD method. This cross-seeding of common ligands to both data sets [HSA and carbon nanotube] was used to help establish self-consistency across the overall set of binding estimations.

The following features, based upon the carbon nanotube, were considered as constraints to introduce diversity into the set of additional ligands used for binding simulations studies to the carbon nanotube;

- a. The carbon nanotube is very rigid. Hence, relatively flexible ligands should ‘fit’ onto the surface of the nanotube better than rigid ligands.
- b. The carbon nanotube is nonpolar. A ligand having an appreciable complementary nonpolar surface to the nanotube should, therefore, bind well to the nanotube in a surrounding aqueous medium. Strong binding can be maintained if there are polar groups on the ligand that interact with solvent away from the nanotube-nonpolar ligand interface.
- c. Each ligand should be a biologically relevant compound. That is, the ligand should be a drug or a small, naturally occurring, biologically active compound. The range in type of biological response/activity should be diverse across the ligands.

Results

The set of HSA ligands, and their observed and estimated binding affinities to HSA, expressed as $\log k_b$ with k_b being the binding equilibrium constant, are given in Table 1. An increase of $\log k_b$ corresponds to an increase in binding affinity. Figure 1 shows propofol bound at its low concentration HSA binding site as determined from the MM-PBSA MD method employing the crystal structures of free and propofol bound HSA as initial MD simulation structures²². Only the residues that form the ‘lining’ of the propofol-HSA binding site are shown in Figure 1.

The linear correlation equation between the observed $\log k_b$ and the estimated $\log k_b$ of the ligands to HSA is given by;

$$\log k_b (\text{obs}) = 0.827 \log k_b (\text{est}) - 0.121 \quad (2)$$

$N=8 \quad R^2=0.888 \quad Q^2=0.603$

An inspection of Part B of Table 1 reveals that the estimated and observed $\log k_b$ of the ligands generally differ in absolute value by less than one [a factor of 10 in k_b] with

ibuprofen being the largest outlier. A plot of the estimated versus observed $\log k_b$ values is given in Fig. 2 where it is seen that each estimated $\log k_b$ value is larger than the observed value for each ligand. An $R^2 = 0.89$ in eq. (2) indicates that the estimated $\log k_b$ captures about 90% of the variance in the observed $\log k_b$ over a range in binding of nearly four orders of magnitude. Thus, it is reasonable to postulate that the application of the methodology employed for estimating ligand-HSA binding, including the MM-PBSA approach, can be applied to at least differentiate strong and weak binding ligands to a carbon nanotube. In addition, the estimated magnitude of binding of a ligand to a carbon nanotube can be meaningfully compared to the range in estimated binding constants of known ligands to HSA.

Table 2 reports the chemical structures along with the use and function of a set of selected polar and/or rigid ligands whose chemical structures were selected to introduce diversity with respect to the three constraints presented in Section E of **Methods**. These ligands would not be expected to bind particularly well to the carbon nanotube based upon constraints *a*) and *b*) and chemical intuition.

A set of nonpolar and/or flexible ligands, whose chemical structures are shown in Table 3, have also been chosen as binding candidates to a carbon nanotube. These ligands have chemical structures which are conducive to binding to the carbon nanotube based on constraints *a*) and *b*) given in Section E of **Methods**.

Table 4 contains the composite set of 23 ligands described in Tables 1 – 3 whose binding potencies to a carbon nanotube, as measured by $\log k_b$, have been determined by applying the MM-PBSA MD method and eq. (2). Part A of Table 4 includes the ligands of Table 1 which are also observed to bind to HSA. Part B of Table 4 reports the calculated $\log k_b$ values of the set of selected polar and/or rigid ligands given in Table 2, and Part C of Table 4 reports the calculated $\log k_b$ to a carbon nanotube of the set of nonpolar and/or flexible ligands given in Table 3.

The HSA Ligands

Each of the HSA ligands, except for ibuprofen, is calculated to bind less strongly to a carbon nanotube than is correspondingly both observed and estimated to HSA, see Table 2. Ibuprofen is estimated, using eq.2, to bind more strongly to a carbon nanotube than is observed for its binding to HSA, and about the same as its estimated $\log k_b$ to HSA based upon eq.2. However, ibuprofen is the major outlier in the set of ligands whose estimated binding to HSA is known, see Table 1, Part B. Moreover, ibuprofen is estimated to bind much more strongly to HSA than observed. Thus, caution is warranted in accepting the absolute estimated high affinity of ibuprofen to the carbon nanotube.

The average observed binding of the eight HSA ligands to HSA is 4.47 with a range of [1.98 to 5.88]. Correspondingly, the average estimated, using eq.2, binding of the eight HSA ligands to a carbon nanotube is 2.99 with a range of [0.25 to 5.90]. Keeping in mind that the sample set of eight ligands is small, these averages and ranges in binding would suggest;

- a. the HSA ligands bind better to HSA than to the carbon nanotube.
- b. the HSA ligands show a wide range in binding to both HSA and the carbon nanotube.
- c. the range in binding to the carbon nanotube is larger than to HSA and arises from some poor binding ligands to the carbon nanotube.

The predicted set of $\log k_b$ values for each of the ligands given in Tables 3 and 4, using both eqs. 1 and 2, are given in Fig. 3.

The preferred binding mode of propofol to a carbon nanotube, based upon the docking procedure employed and the MM-PBSA approach, is shown in Fig. 4b. Figure 4a shows the initial MDS propofol-nanotube docking structure, and in both parts of Fig. 4 the water molecules have been suppressed in the visualization. propofol exhibits little geometric specificity in preferred binding modes to the nanotube. That is, propofol is equally bound in any of a large number of different binding geometries. This situation arises seemingly because both propofol and the carbon nanotube are rigid and there is only one polar hydroxyl group on the otherwise nonpolar and ellipsoidal propofol molecule. Hence, there is little geometric specificity regarding the binding of propofol to the carbon nanotube. The relatively high binding affinity [$\log k_b = 4.57$] of propofol to the nanotube among the eight HSA ligands arises from the rigidity of both the nanotube and propofol. This rigidity results in a small loss in binding free energy due to an entropy change upon binding. The entropy loss, ΔS , including desolvation entropy, of propofol binding to the carbon nanotube is given in Table 5. It is seen that this is the smallest entropy [and, therefore, free energy] change of the three exemplary compounds given in Table 5.

The Rigid and/or Polar Ligands

The average estimated binding of the nine rigid and/or polar ligands, using eq.2, to a carbon nanotube is 4.23 with a range in binding affinity of [1.88 to 6.95]. This is a much higher average binding affinity to the nanotube than determined for the eight HSA ligands to the nanotube [2.99], and not too much different from the average binding of the HSA ligands to HSA [4.47]. The range in estimated $\log k_b$ of over 5 orders of magnitude suggests a marked specificity in binding. This is intuitively surprising as one would have expected all of these compounds to be relatively poor binders based upon their rigidity and/or polarity. Dabigatran is actually predicted to bind at the low-end of the range characteristic of drugs [10^{-7}]³⁵.

Some of these polar and/or rigid molecules, including dabigatran and montelukast, the two compounds predicted to best bind to the carbon nanotube, have sufficient flexibility to snugly fit their nonpolar ‘sides’ onto the nanotube surface. This conformational flexibility is shown by argatroban, an average binder in this class of ligands to the carbon nanotube, in Fig. 5. Part A of Fig. 5 shows argatroban in its preferred solution conformation prior to performing an MDS docking simulation to the carbon nanotube. Part B of Fig. 5 shows argatroban in its preferred bound form to the carbon nanotube. Clearly argatroban has undergone a major conformational change upon binding to the carbon nanotube. In solution argatroban adopts a balled-up, oil-drop conformation to minimize exposure of nonpolar groups to solvent, and maximize polar group interactions with the aqueous media. In the bound state argatroban adopts an open extended conformation in which one ‘side’ of its surface is largely nonpolar and binds to the carbon nanotube, and the other ‘side’ is more polar and exposed to the aqueous media. This conformational change corresponds to only a moderately larger change in ligand binding entropy as compared to propofol, see Table 5, even though the unbound and bound geometries are very different as is evident in Fig. 5.

The Flexible and/or Nonpolar Ligands

The average estimated binding of the six flexible and/or nonpolar ligands, using eq.2, to a carbon nanotube is 5.82 with a range of [4.27 to 7.14], see Table 4, Part C. This is a much higher average binding affinity to the nanotube than is observed for the eight HSA ligands to HSA [4.47]. The range in estimated $\log k_b$ is a bit less than 3 orders of magnitude. Thus, as is intuitively suggested, flexible and/or nonpolar ligands readily bind with considerable strength to a carbon nanotube. Both DMPG and PGI2 are predicted to bind at the low-end of the range characteristic of drugs [10^{-7}]³⁵.

Figure 6 illustrates the lowest free-energy binding mode of PGI₂ to a carbon nanotube with, in this case, the waters of the MDS shown. The suggestion that these types of ligands might bind strongly to a carbon nanotube, owing to their flexible nonpolar chains wrapping around the nanotube, is born out by inspection of Fig.6. It is readily seen, especially in the top view shown in Part B of Fig. 6, how the PGI₂ chain partially coils about the surface of the nanotube in what is marginally the lowest free energy state among many about equally preferred, and near geometrically equivalent, conformations and alignments. And it is also clear, particularly from the side view in Part A of Fig.6, that the polar groups of PGI₂ are exposed to water in the bound state. PGI₂ loses a considerable amount of conformational entropy as compared to both propofol and argatroban, see Table 5, upon binding to the carbon nanotube, but the corresponding loss in free energy is more than compensated by the gain in binding enthalpy.

An inspection of Fig. 6 reveals that there are few waters in direct contact with the carbon nanotube, whereas the aliphatic chains of PGI₂ are directly interfacing with the surface of the nanotube. The rigid nanotube acts as an entropy reservoir to the water molecules leading to a cage-like structure of waters about the nanotube. Water molecules can also migrate into the interior of the nanotube as can be seen in Fig.6, Part B.

Discussion

The principal finding from this study is that several of the drugs and biologically active compounds investigated have estimated binding affinities to carbon nanotubes that fall into the upper range, and beyond, observed for the binding of drugs to HSA. Moreover, a few of the ligands considered in this study are predicted to bind to the carbon nanotube in the 10^{-7} range which is often considered a lower limit of affinity when developing drugs³⁵. Thus, the presence of nanotubes in the body could alter the normal pharmacodynamic profiles of drugs and biologically active compounds.

There are many drugs and small biological molecules that can and should be considered in a study of this type. For example, steroids and related endogenous compounds would be good candidates because of their essential biochemical roles. However, such types of structures were not considered in this initial study because the planar geometry and rigidity of the steroid core would not be expected to interact very significantly with the rigid, cylindrical structure of a carbon nanotube. However, they are many prime candidates for future nanomaterial computational-based binding studies. Also, there is the consideration that the entire bound drug-carbon nanotube complex could bind selectively to a receptor site. However, the large size, high rigidity and geometric shape of a carbon nanotube make it highly unlikely that a bound drug-carbon nanotube complex could perform as a novel ligand to a receptor with any reasonable affinity potency.

It was not possible to identify any experimental data for the binding of any molecule to a carbon nanotube. Discussions with some groups involved in making such binding measurements indicated that attempts to make such affinity measurements had proven very difficult and unreliable owing to the high hydrophobicity of the carbon nanotube. Moreover, it needs to be remembered that a primary reason for doing computational chemistry is to make computational estimations when measurements cannot be made. Thus, this work is putting forth binding predictions in the absence of being able to supply confirmatory experimental measurements.

Unsuccessful attempts were made to develop classic QSAR models for the binding of the ligands of Table 1 — Part A to HSA. Classic QSAR descriptors and modeling cannot seemingly capture the subtle 3D-geometric features, especially for low to medium level

binding affinity events, needed to build a meaningful QSAR model. Moreover, it is our position that the simplicity of the 3D-structure of the carbon nanotube actually requires an even more detailed 3D modeling approach, like MM-PBSA, than is needed for a receptor like HSA, in order to capture information on the sub-angstrom level to permit accurate differentiation in the ligand-receptor binding interactions involving a carbon nanotube.

However, once a validated high-level method like MM-PBSA has been used to predict the $\log k_b$ values for a set of [preferably analog] ligands to a carbon nanotube, the resulting data set can be considered a training set for use in alternate modeling approaches including QSAR analyses. In principle, classic QSAR models might be constructed which could serve as rapid virtual high-throughput screens for evaluating the affinity propensity of members of libraries of compounds to carbon nanotubes.

It is dangerous to speculate why each estimated $\log k_b$ value for each HSA ligand is larger than its corresponding measured value, see Table 1 and Fig. 2. However, it is possible that the HSA-ligand binding simulations are estimating greater changes in solvation free energies in the binding processes than actually occur. This, in turn, may be attributed to too short a simulation time and/or not considering long-range solvation reorganization behavior. Along these lines of reasoning, there is no apparent reason why ibuprofen binding to HSA should be an outlier more so than any of the other ligands studied. It is possible that overestimation of the changes in desolvation free energy in the simulations may be most attenuated for the HSA-ibuprofen system.

PGI₂ is a metabolite of arachidonic acid, and, as such, is a naturally occurring prostaglandin that has potent vasodilatory activity and inhibitory activity of platelet aggregation³¹. PGI₂ has been developed as a drug known as Flolan³⁶.

The *in vitro* half-life of PGI₂ in human blood at 37°C and pH 7.4 is approximately 6 minutes³⁶. Hence, the *in vivo* half-life of PGI₂ in humans is expected to be no greater than 6 minutes. The results of this current study suggest that PGI₂ will strongly bind [in the 10⁻⁷ range] to an exposed carbon nanotube. Thus, it is reasonable to suggest that nanotubes could serve as reservoirs for PGI₂ molecules, and thereby effectively increase the normal half-life of this potent vasodilator and platelet aggregation inhibitor. However, it must be kept in mind that there is little definitive information as to how carbon nanotubes distribute in living systems, including humans.³⁷ One study using mice indicates a bioaccumulation of carbon nanotubes in the body. Another study suggests that uptake of carbon nanotubes into the lung may pose an asbestos-like threat to humans.³⁸ Very recently, strong evidence has been reported that carbon nanotubes can enter into, and migrate about, the interior of human cells.³⁹

Overall, the findings from this study indicate that ligand binding potency to a carbon nanotube is largely controlled by the shape, distribution of polar/nonpolar groups and flexibility of the ligand. Known ligands that bind to HSA exhibit limited binding to a carbon nanotube. These HSA ligands tend to be spherical/ellipsoidal in shape, relatively rigid, small to moderate in size and quite variable in their distributions of polar/nonpolar character. The general rigidity and spherical shape of the HSA ligands seemingly most restrict their binding to a carbon nanotube. The polar and/or rigid ligands bind less strongly to the carbon nanotube, on average, than do the nonpolar and/or flexible ligands even though both classes of ligands have chain-like shapes that facilitate binding. The introduction of only a few strategically spaced single bonds in the polar and/or rigid ligands markedly increases their binding to the carbon nanotube. The ability of a ligand to adopt a low-energy conformation characterized by a nonpolar 'side' and a 'polar side' also facilitates binding to the a carbon nanotube.

Still, the results of this study cannot be meaningfully ‘transferred’ to other nanomaterials for most of the same reasons that findings from one biological ligand-receptor system are not usually representative of another biological ligand-receptor system. The geometries and chemistries involved are sufficiently different between different classes of nanomaterials so as to negate any type of significant extrapolation. Indeed, preliminary results of work we have in progress suggest that simply putting side chains on a carbon nanotube imparts highly distinct properties reflective of the type, location and distribution of the side chains relative to the core carbon nanotube structure.

Acknowledgments

This work was funded by the National Institutes of Health through the NIH Roadmap for Medical Research, Grant 1 R21 GM075775. Information on Novel Preclinical Tools for Predictive ADME-Toxicology can be found at <http://grants.nih.gov/grants/guide/rfa-files/RFA-RM-04-023.html>. Links to nine initiatives are found here <http://nihroadmap.nih.gov/initiatives.asp>. This work was also supported, in part, by The Procter & Gamble Company. Resources of the Laboratory of Molecular Modeling and Design at UNM, and at The Chem21 Group, Inc., were used in performing these studies.

References

1. Donaldson K, Stone V, Tran CL, Kreyling W, Borm PJA. Nanotoxicology. *Occup. Envir. Med.* 2004; 61(9):727–728.
2. Service RF. Nanotoxicology: Nanotechnology grows up. *Sci.* 2004; 304(5678):1732–1734.
3. Symposium abstracts. *Environ. Mol. Mutagenesis.* 2007; Vol. 48:524–549.
4. Fischer HC, Chan WCW. Nanotoxicity: the growing need for in vivo study. *Curr. Opin. Biotech.* 2007; 18(6):565–571. [PubMed: 18160274]
5. Zhao Y, Xing G, Chai Z. Nanotoxicology: Are carbon nanotubes safe? *Na.t Nano.* 2008; 3(4):191–192.
6. Genaidy, W. K. Ash Nanotechnology occupational and environmental health and safety: Education and research needs for an emerging interdisciplinary field of study. *Human Factors and Ergonomics in Manufacturing.* 2006; 16(3):247–253.
7. Service RF. US nanotechnology - Health and safety research slated for sizable gains. *Sci.* 2007; 315(5814):926–926.
8. Lam CW, James JT, McCluskey R, Arepalli S, Hunter RL. A review of carbon nanotube toxicity and assessment of potential occupational and environmental health risks. *Crit. Rev. Toxicol.* 2006; 36(3):189–217. [PubMed: 16686422]
9. Shvedova AA, Castranova V, Kisin ER, Schwegler-Berry D, Murray AR, Gandelsman VZ, Maynard A, Baron P. Exposure to carbon nanotube material: Assessment of nanotube cytotoxicity using human keratinocyte cells. *J. Tox. Envir. Health-Part A.* 2003; 66(20):1909–1926.
10. Hilder TA, Hill JM. Theoretical comparison of nanotube materials for drug delivery. *Micro. Nano. Let., IET.* 2008; 3(1):18–24.
11. Kostarelos K. The long and short of carbon nanotube toxicity. *Nature Biotech.* 2008; 26(7):774–776.
12. Poland CA, Duffin R, Kinloch I, Maynard A, Wallace WAH, Seaton A, Stone V, Brown S, MacNee W, Donaldson K. Carbon nanotubes introduced into the abdominal cavity of mice show asbestos-like pathogenicity in a pilot study. *Nat. Nano.* 2008; 3(7):423–428.
13. Chakravarty P, Marches R, Zimmerman NS, Swafford ADE, Bajaj P, Musselman IH, Pantano P, Draper RK, Vitetta ES. Thermal ablation of tumor cells with antibody-functionalized single-walled carbon nanotubes. *Proceed. Natl. Acad. Sci.* 2008; 105(25):8697–8702.
14. Liu Z, Davis C, Cai W, He L, Chen X, Dai H. Circulation and long-term fate of functionalized, biocompatible single-walled carbon nanotubes in mice probed by Raman spectroscopy. *Proceed. Natl. Acad. Sci.* 2008; 105(5):1410–1415.
15. Monteiro-Riviere NA, Nemanich RJ, Inman AO, Wang YY, Riviere JE. Multi-walled carbon nanotube interactions with human epidermal keratinocytes. *Tox. Let.* 2005; 155(3):377–384.

16. Witzmann FA, Monteiro-Riviere NA. Multi-walled carbon nanotube exposure alters protein expression in human keratinocytes. *Nanomedicine*. 2006; 2(3):158–168. [PubMed: 17292138]
17. Guo L, Bussche AVD, Buechner M, Yan A, Kane AB, Hurt RH. Adsorption of Essential Micronutrients by Carbon Nanotubes and the Implications for Nanotoxicity Testing. *Small*. 2008; 4(6):721–727. [PubMed: 18504717]
18. Hummer G, Rasaiah JC, Noworyta JP. Water conduction through the hydrophobic channel of a carbon nanotube. *Nature*. 2001; 414(6860):188–190. [PubMed: 11700553]
19. Lopez CF, Nielsen SO, Moore PB, Klein ML. Understanding nature's design for a nanosyringe. *Proceed. Natl. Acad. Sci.* 2004; 101(13):4431–4434.
20. Liu J, Hopfinger AJ. Identification of Possible Sources of Nanotoxicity from Carbon Nanotubes Inserted into Membrane Bilayers Using Membrane Interaction Quantitative Structure–Activity Relationship Analysis. *Chem. Res. Toxicol.* 2008; 21(2):459–466. [PubMed: 18189365]
21. Wermuth, CM. *The Practice of Medicinal Chemistry*. 2nd ed. Academic Press; London: 2003.
22. Bhattacharya AA, Curry S, Franks NP. Binding of the general anesthetics propofol and halothane to human serum albumin - High resolution crystal structures. *J.f Biol. Chem.* 2000; 275(49): 38731–38738.
23. Ghuman J, Zunszain PA, Petitpas I, Bhattacharya AA, Otagiri M, Curry S. Structural basis of the drug-binding specificity of human serum albumin. *Journal of Mol. Biol.* 2005; 353(1):38–52. [PubMed: 16169013]
24. Tozer, TN.; Rowland, M. *Introduction to Pharmacokinetics and Pharmacodynamics: The Quantitative Basis of Drug Therapy*. 1st ed. Lippincott Williams & Wilkins; 2006.
25. Kollman PA, Massova I, Reyes C, Kuhn B, Huo S, Chong L, Lee M, Lee T, Duan Y, Wang W, Donini O, Cieplak P, Srinivasan J, Case DA, Cheatham TE. Calculating Structures and Free Energies of Complex Molecules: Combining Molecular Mechanics and Continuum Models. *Acc. Chem. Res.* 2000; 33(12):889–897. [PubMed: 11123888]
26. Case, DA.; Darden, TA.; Cheatham, TE., III; Simmerling, CL.; Wang, JD.; R., E.; Luo, R.; Merz, KM.; Pearlman, DA.; Crowley, MW.; R., C.; Zhang, W.; Wang, B.; Hayik, S.; Roitberg, A.; Seabra, G.; Wong, KF.; Paesani, F.; Wu, X.; Brozell, S.; Tsui, V.; Gohlke, H.; Yang, L.; Tan, C.; Mongan, J.; Hornak, V.; Cui, G.; Beroza, P.; Mathews, DH.; Schafmeister, C.; Ross, WS.; Kollman, PA. *AMBER 9*. 9th ed. University of California; San Francisco: 2006.
27. Pearlman DA, Case DA, Caldwell JW, Ross WS, Cheatham TE, DeBolt S, Ferguson D, Seibel G, Kollman P. *AMBER*, a package of computer programs for applying molecular mechanics, normal mode analysis, molecular dynamics and free energy calculations to simulate the structural and energetic properties of molecules. *Computer Phys. Comm.* 1995; 91(1-3):1–41.
28. O'Neil, MJ.; Smith, A.; Heckelman, PE.; Budavari, S. *The Merck Index*. 13th ed. Merck Publishing Group; Whitehouse Station, N.J., USA: 2006.
29. Liu J, Yang L, Li Y, Pan D, Hopfinger A. Prediction of plasma protein binding of drugs using Kier—Hall valence connectivity indices and 4D-fingerprint molecular similarity analyses. *J. Computer-Aided Mol. Design*. 2005; 19(8):567–583.
30. Hauptmann J. Pharmacokinetics of an emerging new class of anticoagulant/antithrombotic drugs - A review of small-molecule thrombin inhibitors. *Eur. J. Clin. Pharm.* 2002; 57(11):751–758.
31. Weeks JR. General Pharmacology of Prostacyclin, (PGX) - New prostaglandin especially active on cardiovascular system. *Acta Biol. Medica Germanica*. 1978; 37(5-6):707–714.
32. Pascher I, Sundell S, Harlos K, Eibl H. Conformation and packing properties of membrane lipids: the crystal structure of sodium dimyristoylphosphatidylglycerol. *Biochim. Biophys. Acta Biomembr.* 1987; 896:77–88.
33. Bradshaw JP, Bushby RJ, Giles CCD, Saunders MR. Orientation of the headgroup of phosphatidylinositol in a model biomembrane as determined by neutron diffraction. *Biochem.* 1999; 38(26):8393–8401. [PubMed: 10387085]
34. Hauser H, Pascher I, Pearson RH, Sundell S. Preferred conformation and molecular packing of phosphatidylethanolamine and phosphatidylcholine. *Biochim. Biophys. Acta*. 1981; 650:21–51. [PubMed: 7020761]
35. Williams, DA.; Lemke, TL.; Foye, WO. *Foye's Principles of Medicinal Chemistry*. 5th ed. Lippincott Williams & Wilkins; New York: 2002.

36. accessed 12/18/2008 <http://www.rxlist.com/flolan-drug.htm>
37. accessed 12/21/2008 www.nature.com/nchina/2008/080409/full/nchina
38. accessed 12/20/2008 www.naturalnews.com/024215.html
39. accessed 12/20/2008 www.physorg.com/news114348754.html

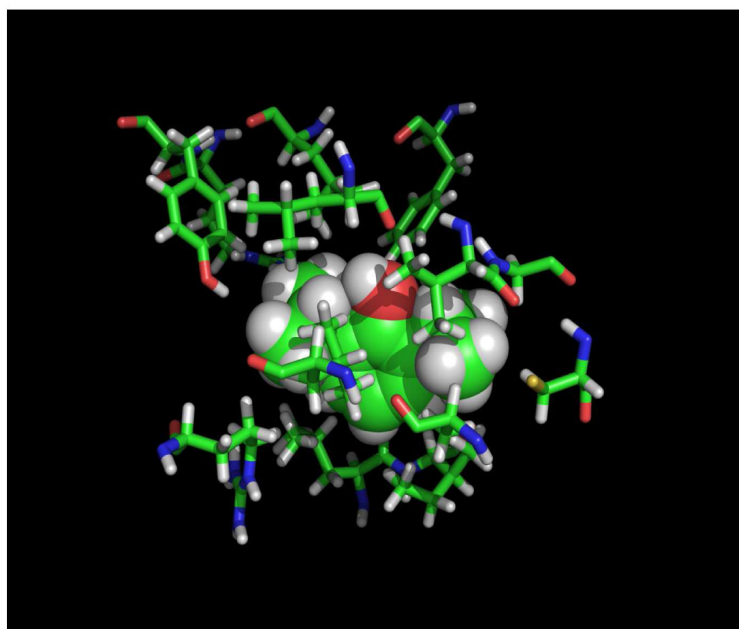


Figure 1. The bound form of propofol in its low concentration binding site on HSA following MDS. Only the residues forming the ‘lining’ of the binding site are shown and visualization of the waters has been suppressed.

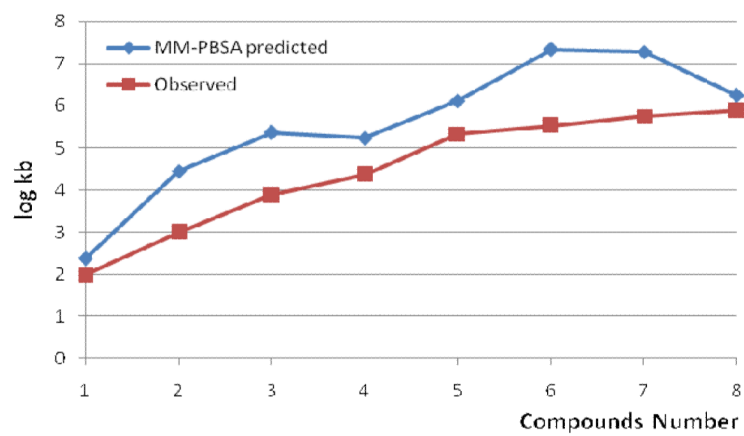


Figure 2.
The observed versus estimated $\log_k b$ values for the HSA ligands

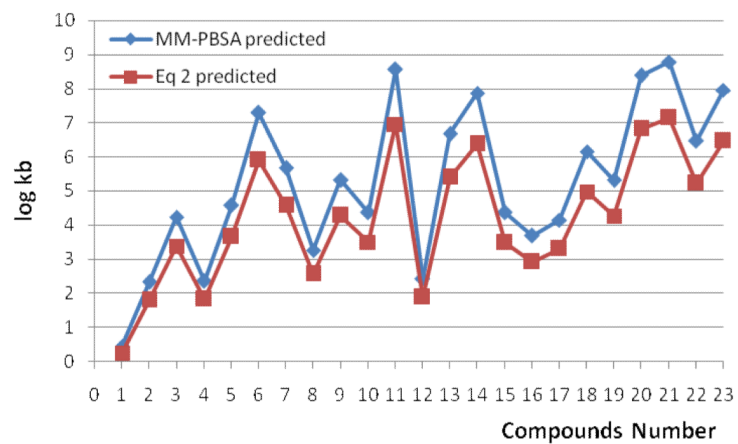
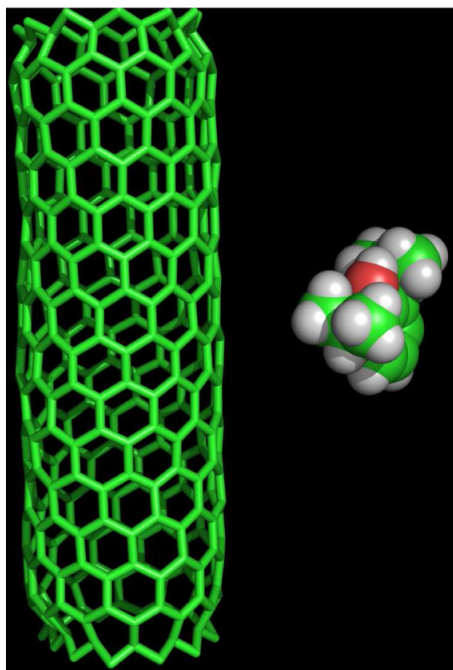
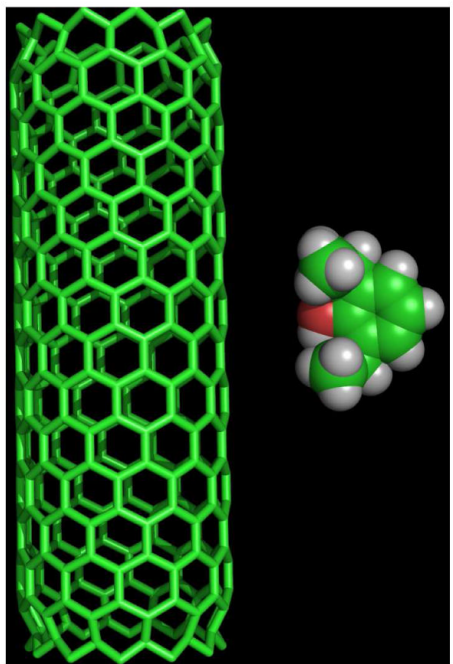


Figure 3. The predicted $\log k_b$ values for the 23 compounds listed in Tables 3 and 4. Both eq. 1 and eq. 2 have been used to make the estimation of $\log k_b$ values.



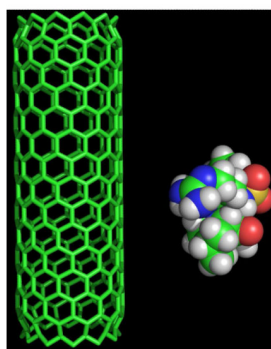
Part A



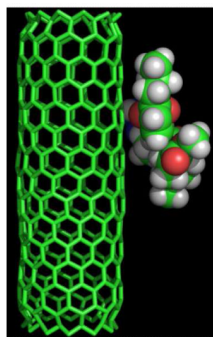
Part B

Figure 4.

The binding of propofol to a carbon nanotube. Part A — Initial geometry before the MDS leading to the lowest energy complex. Part B — Lowest energy geometry realized over the MDS. Visualization of the water molecules has been suppressed.



Part A



Part B

Figure 5. Simulation of argatroban binding to a carbon nanotube. Part A — Preferred solution conformation before the MDS leading to the lowest energy complex. Part B - Lowest energy geometry of the bound complex realized over the MDS. Visualization of the water molecules has been suppressed.

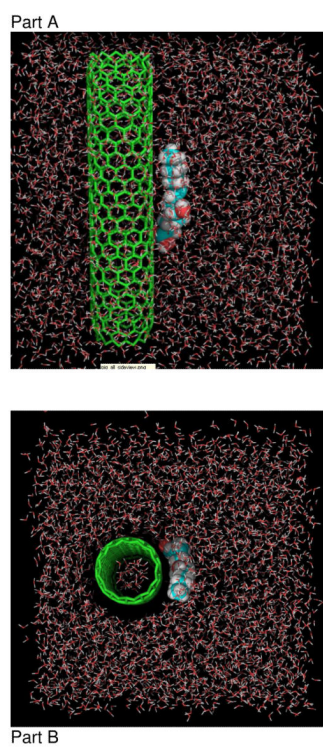
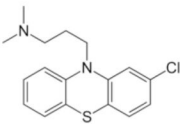
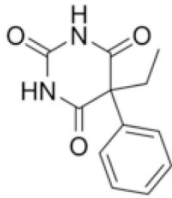
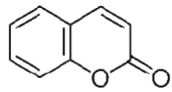
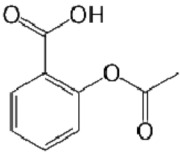
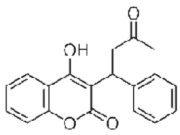
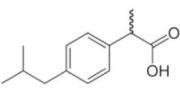
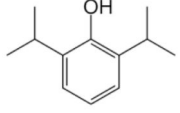
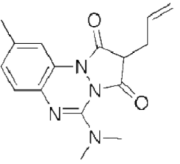


Figure 6. Lowest free energy docking geometry from the MDS of PGI2 binding to a nanotube with the water environment shown. Part A - side-view. Part B - top-view.

Table 1

The chemical structures of the set of HSA ligands, Part A, and their observed and estimated binding affinities to HSA as expressed by $\log k_b$, Part B

Part A			
Comps. #	Ligand Name	Structure	Function
1	Chlorpromazine ²⁸		Antipsychotic
2	Phenobarbital ²⁸		Anticonvulsant
3	Coumarin ²⁹		Precursor for anticoagulants
4	Aspirin ²⁸		Analgesic
5	Warfarin ²⁸		Anticoagulant
6	Ibuprofen ²³		NSAID
7	Propofol ²²		Anesthetic
8	Azapropazone ²³		NSAID

Part B

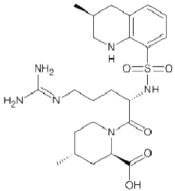
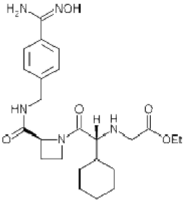
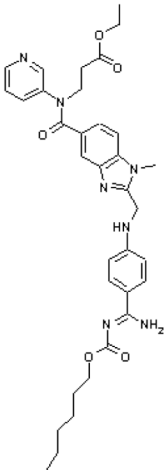
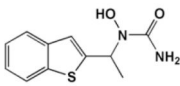
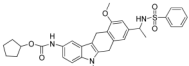
Ligand	$\log k_b$ to HSA	
	Estimated value by the MM—PBSA method	Observed Value
Chlorpromazine	2.37	1.98
Phenobarbital	4.45	3.00
Coumarin	5.36	3.89
Aspirin	5.23	4.37
Warfarin	6.12	5.33
Ibuprofen	7.33	5.52
Propofol	7.28	5.75
Azapropazone	6.25	5.88

Note: NSAID- Non-steroidal anti-inflammatory drug

The text notes the crystal structures of HSA with bound ligand

Table 2

The chemical structures of polar and/or rigid ligands used in the nanotube binding affinity studies applying the MMPBSA method

Comps. #	Comps. Name	Structure	Function
9	Argatroban30		thrombin inhibitor
10	Ximelagatran30		thrombin inhibitor
11	Dabigatran30		thrombin inhibitor
12	Zileuton28		leukotriene blocker
13	Zafirlukast28		leukotriene receptor antagonist

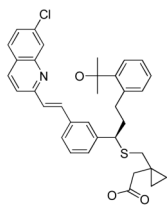
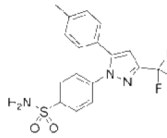
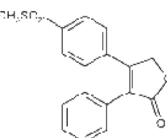
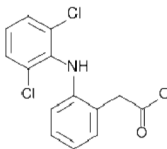
Comps. #	Comps. Name	Structure	Function
14	Montelukast ²⁸		leukotriene receptor antagonist
15	Celecoxib ²⁹		NSAID
16	Rofecoxib ²⁹		NSAID
17	Diclofenac ²⁹		NSAID

Table 3

The chemical structures of nonpolar and/or flexible ligands used in the nanotube binding affinity studies applying the MM-PBSA method

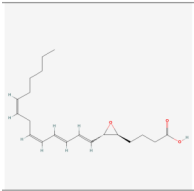
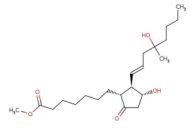
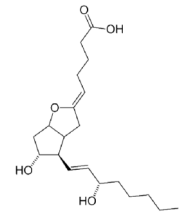
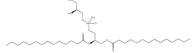
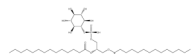
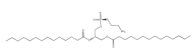
Comps. #	Comps. Name	Structure	Function
18	Leukotriene ₂₈		Eicosanoid lipid mediators
19	Misoprostol ₂₈		Antiulcer & Abortifacient
20	Epoprostenol (PGI ₂ , prostacyclin) ₃₁		Treat pulmonary hypertension
21	DMPG (dimyristoyl-phosphatidylglycerol) ₃₂		Phospholipid
22	DMPI (dimyristoyl-phosphatidylinositol) ₃₃		Phospholipid
23	DMPE (1,2-dimyristoyl-sn-glycero-phosphatidylethanolamine) ₃₄		Phospholipid

Table 4

The set of carbon nanotube ligands and their estimated binding affinities to a carbon nanotube as expressed by $\log k_b$

Part A — The HSA Ligand Set		
Ligand	$\log k_b$ (MM—PBSA method)	$\log k_b$ (eq. 2)
Chlorpromazine	0.45	0.25
Phenobarbital	2.33	1.80
Coumarin	4.23	3.38
Aspirin	2.35	1.82
Warfarin	4.58	3.66
Ibuprofen	7.29	5.90
Propofol	5.67	4.57
Azapropazone	3.26	2.57

Part B — The Polar and/or Rigid Ligand Set		
Ligand	$\log k_b$ (MM—PBSA method)	$\log k_b$ (eq. 2)
Argatroban	5.32	4.28
Ximelagatran	4.37	3.49
Dabigatran	8.56	6.95
Zileuton	2.42	1.88
Zafirlukast	6.68	5.40
Montelukast	7.87	6.38
Celecoxib	4.36	3.48
Rofecoxib	3.68	2.92
Diclofenac	4.14	3.30

Part C — The Nonpolar and Flexible Ligand Set		
Ligand	$\log k_b$ (MM—PBSA method)	$\log k_b$ (eq. 2)
Leukotriene	6.15	4.97
Misoprostol	5.31	4.27
PGI2	8.39	6.82
DMPG	8.78	7.14
DMPI	6.47	5.23
DMPE	7.96	6.46

Table 5

The change in entropy, ΔS , upon binding to a carbon nanotube of the three exemplary ligands discussed in the text. ΔS includes desolvation of the binding process

Ligand	ΔS (cal/mole/deg K)
Propofol	15.1
Argatroban	25.4
PGI2	53.4